Experimental study of the effect of disorder on DNA dynamics in post arrays during electrophoresis

Daniel W. Olson and Kevin D. Dorfman

Phys. Rev. E **86**, 041909 — Published 12 October 2012

DOI: 10.1103/PhysRevE.86.041909

Experimental study of the effect of disorder on DNA dynamics in post arrays during electrophoresis

Daniel W. Olson[1] and Kevin D. Dorfman[1,*]

[1]*Department of Chemical Engineering and Materials Science,*
University of Minnesota — Twin Cities,
421 Washington Ave. SE, Minneapolis, MN 55455

Abstract

We used top-down fabrication techniques to create both an ordered hexagonal array and a disordered array of 1 μm diameter cylindrical posts in a silicon dioxide microchannel with the same number of posts per unit area. The electrophoretic mobility and dispersion coefficient of λ DNA in each of the arrays were obtained as a function of the electric field using ensembles of DNA molecules in a double channel device that minimizes experimental artifacts. To deepen our understanding of the transport, we also used fluorescence microscopy to examine the dynamics of single DNA molecules as they interact with the arrays at a fixed value of the electric field. Based on the results of these two types of experiments, we conclude that the electrophoretic mobility is not dependent on the array order but that band broadening in the device is greater in the disordered array.

PACS numbers: 87.15.hj, 87.14.gk, 47.57.Ng

*Electronic address: dorfman@umn.edu

I. INTRODUCTION

Two dimensional arrays of micron-sized cylindrical posts are proven to rapidly separate long DNA under a dc electric field [1–8]. While the application of a dc electric field using the standard separation matrices (polyacrylamide or agarose gels) fails to produce a size dependent mobility for long DNA ($\gtrsim$10 kbp) [9], the increased pore size of microfabricated arrays results in a size dependent mobility for long DNA. Repeating a regular pattern of posts over a large distance in a microfluidic channel is one method for producing the requisite post array geometry [1–6, 10, 11]. Alternatively, self-assembled magnetic bead arrays, formed by the application of a magnetic field to a suspension of super-paramagnetic beads in a microfluidic channel, also produce the necessary geometry to separate long DNA by size [7, 8]. In both types of arrays, DNA collides with the individual posts of the array and disengages with a time that depends on the size of the DNA molecule [12–14]. A schematic of DNA colliding with the posts of the array is shown in Fig. 1. Significant spatial separation of different species requires many collisions during transport in the device [12].

Initial simulations of DNA transport in ordered and disordered post arrays using a 2D bead-rod model suggested that disordered post arrays result in lower electrophoretic mobility than ordered square and hexagonal arrays [15]. In the ordered arrays, DNA molecules migrate in the 'channel' between the edges of posts, which leads to fewer DNA-post collisions. Further simulations, using a 3D bead-spring model for DNA, also found that very few collisions occur in an ordered post array [16]. The dispersion coefficient in ordered arrays thus approaches the free solution diffusion coefficient of the DNA as there are very few DNA-post collisions. The results of these studies suggested that disordered arrays are essential to size separation due to an increased collision probability. It should be noted that both studies neglected perturbations to the electric field caused by the presence of the posts. These perturbations are shown in Fig. 1 for the geometries used in the present study.

In contrast to the predictions of these simulations, experimental observations of DNA electrophoresis in a hexagonal array of 1 μm diameter posts with 3 μm center-to-center spacing showed that frequent DNA-post collisions *do* occur in an ordered array at this post density [17]. Moreover, Brownian dynamics simulations that included the perturbations in the electric field caused by insulating posts matched the experimentally measured electrophoretic mobility [17, 18], indicating that the disturbance in the electric field due to the

posts qualitatively alters the transport in this relatively tight array. These experiments and simulations showed that DNA makes enough collisions in an ordered array to yield a size based separation [19]. However, it is still unclear whether an ordered or disordered array will be superior for long DNA separation. Since Brownian dynamics simulations of DNA transport in post arrays have given conflicting results on the utility of ordered arrays, an experimental study is necessary to definitively determine the role of order in post arrays. In the following, we examine the role of disorder on the transport properties of long DNA, thereby providing a fundamental basis to determine the role of disorder on DNA size separation.

The two most important measures of separation efficacy are the time to conduct the separation and the resulting separation resolution. The separation resolution is defined as

$$R_s = \frac{\Delta\mu}{\langle\mu\rangle}\sqrt{\frac{L}{16H}}, \tag{1}$$

where $\Delta\mu$ is the difference in electrophoretic mobility between two species, $\langle\mu\rangle$ is their average mobility, L is the length of the separation device, and H is the plate height. The plate height is a macroscopic measurement of microtransport properties and can be written as $H = 2\bar{D}/\bar{U}$, where $\bar{D}$ is the dispersion coefficient in the array and $\bar{U}$ is the averaged velocity in the array. We are interested here in determining whether the factors appearing in Eq. 1, namely the electrophoretic mobility and the plate height, are affected by disorder in the array. As such, it proves sufficient to study the dynamics of a single DNA size with a molecular weight typically used in the separations. In this manner, we can unambiguously ascertain the changes in electrophoretic mobility and plate height without introducing artifacts inherent in multicomponent data, such as deconvolving overlapping peaks. We thus measured the electrophoretic mobility of λ DNA (48.5 kbp) in an ordered post array and a disordered post array to determine whether the mobility depends on the array type. Observations of DNA-post collisions in each array type revealed the cause of the deviation between the free solution mobility and the mobility inside the array. As shown in Eq. 1, resolution is maximized by minimizing plate height. We thus measured the plate height of a single species in both array types and determined the underlying causes of band broadening from single molecule observations. Because the time to conduct the separation is directly proportional to the applied electric field, we further measured DNA velocity and band broadening over a wide range of electric fields. Based on our measurements, we provide guidelines for optimizing the array and electric field.

II. MATERIALS AND METHODS

The ordered array in Fig. 1A consists of 1 μm diameter cylindrical posts with a 5 μm center-to-center spacing in a regular hexagonal pattern. To create the disordered array in Fig. 1B, we allowed each post of the regular hexagonal array to undergo a short random walk consisting of $n = 15$ steps with a distance of $d = 0.5$ μm and a random angle. We characterized the disorder of the array by the dimensionless dispersion of the array, s, that corresponds to the deviation of the array from a regular hexagonal array [13]. For the random walk described above, the dispersion of the array is given by

$$s = \frac{d}{a}\sqrt{n}, \tag{2}$$

where $a = 5$ μm is the center-to-center spacing of the ordered array. Using Eq. 2, the theoretical dispersion of the disordered array is $s = 0.387$. The parameters for the random walk were chosen to provide substantial disorder in the array while keeping the posts far enough from each other to allow fabrication of individual posts.

A. Single Molecule Experiments in a 2-Reservoir Device

We fabricated a 2-reservoir device with 50 rows of an ordered array and 50 rows of a disordered array in series. The two arrays were separated by a post free region 2 mm long. The device is shown schematically in Fig. 2. We fabricated the device in oxidized silicon using projection lithography following a procedure described previously [20]. We characterized the chip by SEM (Fig. 3A,B) after oxidation to confirm that each post has a diameter of 1 μm and to make the measurement of the disorder of each array described above. The oxidized wafer was bonded to a 100 micron thick BOROFLOAT wafer (Mark Optics) by anodic bonding at 450°C and 1800 V. We scored and cracked the wafer into individual devices. The sealed channel was attached to a glass backplate and plastic reservoirs (Upchurch Scientific) with NOA 81 optical adhesive (Norland Products).

We dyed λ DNA (48,502 bp, New England Biolabs) with the fluorescent dye YOYO-1 (Molecular Probes) at a ratio of one dye molecule to eight bp of DNA. At this dye ratio, YOYO-1 bisintercalation into the DNA backbone saturates and external binding to the DNA molecule begins [21]. We have found that a relatively high dye ratio is useful for high spatial and temporal resolution of single molecules based on our previous work [18, 22]. While such

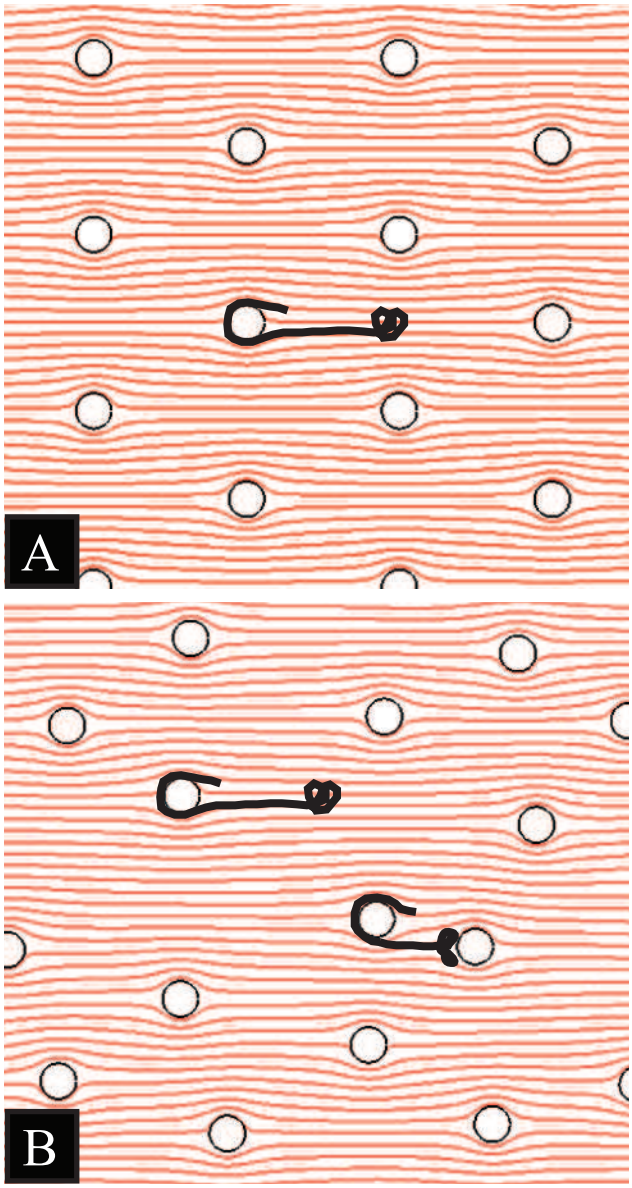

FIG. 1: (Color online) Schematic of a DNA molecule colliding in the ordered array (A) and DNA molecules colliding in the disordered array (B). In the disordered array, DNA can collide with an isolated post or with multiple posts in a single collision event. Red lines approximate the electric field lines in each array.

a high dye ratio was not necessary for data acquisition in the 5-reservoir device, we used a constant dye ratio for both the single molecule and the ensemble level experiments to facilitate comparison between them.

Prior to DNA loading, we filled one reservoir of the channel with a solution of 1 wt% polyvinylpyrrolidone (PVP) in DI water and loaded the channel using a syringe pump for one

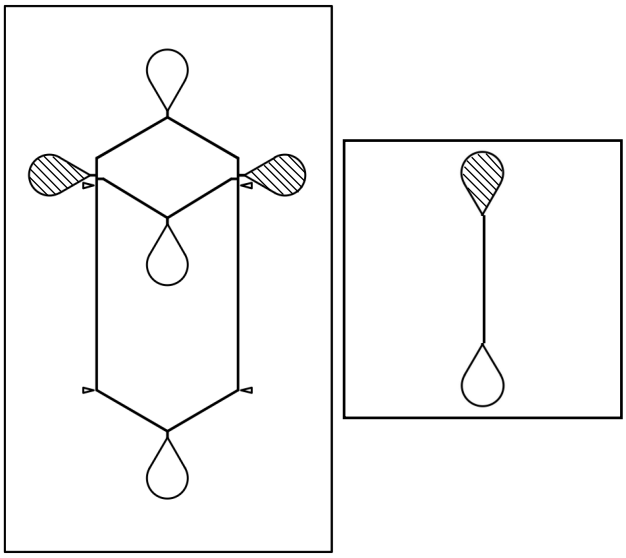

FIG. 2: Schematics for the devices used in the experiments. The 5-reservoir chips is shown on the left, and the 2-reservoir chip on the right. DNA is loaded into the hashed reservoirs and driven through the device by an applied electric field. The 5-reservoir chip contains the ordered array in the left channel and the disordered array in the right channel. Post arrays span the channel between the arrows. 50 rows of the ordered array and disordered array are placed in the 2-reservoir array.

hour. Neutral, adsorbed polymers suppress electroosmotic flow (EOF) during electrophoresis by forming a dynamic surface coating [23]. While several polymers have been shown to reduce EOF in capillaries [24], we chose PVP based on its success in microfluidic devices [1, 5, 6, 14, 18, 20, 22, 25, 26]. The device can be conditioned with the polymer overnight to develop a uniform surface coating [22, 27, 28]; however, several groups have had success conditioning the device for less than one minute [24], or simply including polymer in the running buffer [6, 14, 20, 25, 26]. Our one hour conditioning time is sufficient for EOF suppression and has been reported elsewhere [5, 18, 29].

We then equilibriated the channel with a running buffer of 2.2x TBE, supplemented with 0.07 wt% PVP, 0.07 wt% ascorbic acid, which was pumped into the channel with a syringe pump for one hour. The high salt concentration of this buffer reduces the size of the electric double layer and is commonly used in microfluidic electrophoresis experiments [14, 17, 18, 20, 22, 25, 26]. Before DNA loading, we heated 200 μL of a solution of approximately 0.1 μg/mL

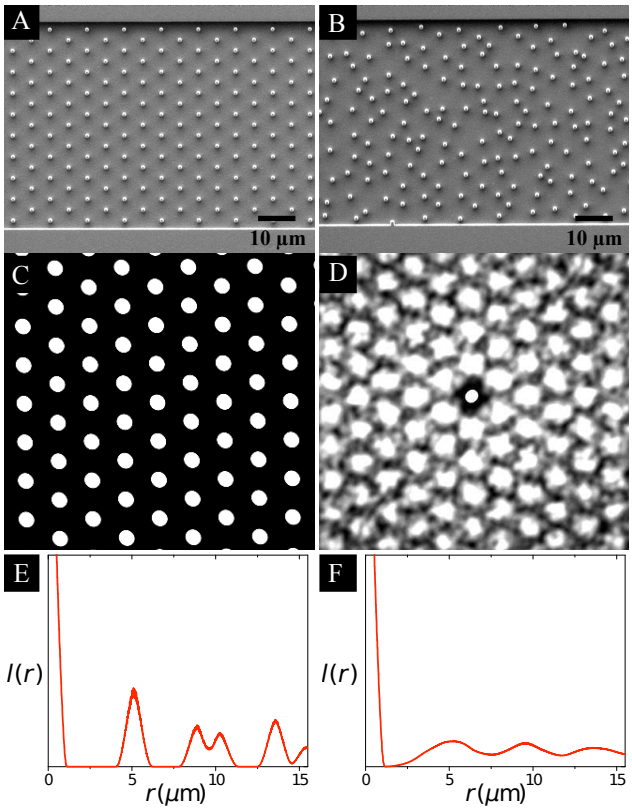

FIG. 3: (Color online) Scanning Electron Micrographs of the oxidized array geometry for the ordered hexagonal array (A) and the disordered array (B). 2D autocorrelation function of the binary SEM image of the ordered array (C) and of the disordered array (D). Radial intensity function of the ordered array (E) and disordered array (F). The autocorrelation function and radial intensity functions are discussed in section IV A.

λ DNA in running buffer at 70°C for 15 minutes to melt any λ DNA concatemers to single, linear λ DNA molecules. A potential difference of 10 V was applied across the 1 cm long channel using platinum electrodes and a Trek power supply (Model 677B), corresponding to a nominal electric field of 10 V/cm. Images were captured on an EM-CCD camera (Photometrics Cascade II) at 25 frames per second using a 100x, 1.4 NA, oil immersion objective on an inverted epifluorescence microscope (Leica DMI 4000B).

We analyzed the single molecule data in the context of the two-state continuous-time random walk (CTRW) model [19]. To measure the hold-up time, we fixed the observation window at the end of each post array and recorded tif stacks with 0.04 second exposure time. We were able to observe a length of the array equivalent to 18 rows of posts. We analyzed

the video microscopy data using an automated tracking program as described previously [18]. To find the probability distribution of the distance between collisions (x) we needed to observe a collision pair from a large fraction of the molecules. While this measurement was possible in a 3 μm spacing array using a stationary stage [18], the decreased post density studied here led to an increase in x. To measure collision pairs we needed to increase the length of the viewing window. We automated the stage using Micro-Manager to follow the DNA molecules as they travel through the post array. The viewing window began at the array entrance and moved the equivalent of 9 rows of posts 4 times to follow individual DNA molecules through the whole post array. The timing of the stage jumps was determined by the average DNA velocity in the array. Using this method we were able to track individual molecules over an expanded viewing window of 50 rows of posts. Photo-bleaching of the DNA molecules limits the measurement of this distance at an applied field of 10 V/cm. We located DNA-post collisions in the moving stage videos manually using the 4-quadrant definition of a collision [25]. We measured the total intensity of each molecule to ensure that it is λ-DNA and not a small fragment of DNA. The cumulative probability density does not go to unity because some molecules do not make a second collision in the array.

B. Velocity and Dispersion Measurements in a 5-Reservoir Device

The DNA electrophoretic mobility (μ) remains relatively constant in a single day of experiments but normally varies over different days of experiments due to environmental factors [5]. In order to measure mobility simultaneously in different geometries during a single experiment, and thus avoid the error due to day-to-day variations, we designed a 5-reservoir device with 15 mm ordered and 15 mm disordered arrays side-by-side in oxidized silicon (Fig. 2). A single experiment in this device greatly reduces variations in mobility because (i) all surfaces in the device receive the same pretreatment; (ii) buffer conditions are identical; (iii) background electro-osmotic flow is constant; and (iv) other uncontrolled variables (temperature, etc.) are the same for the ordered and disordered arrays.

The 5-reservoir device was fabricated as described previously [20] with two exceptions; the photolithography step and device assembly. Instead of projection lithography, we used standard photolithography (Karl Suss MA-6) with S1805 photoresist (Shipley). The device was anodically bonded to 500 μm thick BOROFLOAT glass as this thicker glass is easier to

handle and DNA was not imaged with high numerical aperture objectives in this device. The assembled device was sealed into a polycarbonate chip holder which increased the reservoir volume to 200 μL.

We injected a plug of λ DNA into the ordered and disordered arrays simultaneously and scanned each channel using an automated stage (Prior Scientific) mounted on an inverted epifluorescence microscope (Leica). The 5-reservoir device has two DNA loading reservoirs that are connected with common buffer supply and waste reservoirs by two shifted T injection areas. Voltage was set at each of the five reservoirs by a platinum electrode connected to a high voltage power supply. The electric field was calculated by Kirchoff's Law assuming a constant resistance in all channels of the device. This assumption is valid because the post density is very low; 93% of the volume of the post array contains the buffer solution. A photomultiplier tube imaged the fluorescent DNA to record intensity versus time. We used MATLAB to calculate the DNA intensity as a function of distance from the injection. An example of the intensity versus position data is shown in Fig. 4. The channel scanning method gave us a measurement of DNA intensity versus position once every 15 seconds. We calculated the velocity of DNA from the best-fit line of the peak location versus time. For each time point, we also measured the full-width at half-max (FWHM) of the peak, which is related to the standard deviation of a Gaussian peak by FWHM $= \sigma\sqrt{8\ln(2)}$. We calculated the dispersion coefficient ($\bar{D}$) from the best-fit line to the variance versus time according to $\sigma^2 = 2\bar{D}t$. We found that $\bar{D}$ calculated from FWHM was more accurate than $\bar{D}$ calculated from a direct measurement of the variance due to noise in the intensity measurement and the error in the tails of the fit. All linear regression fitting resulted in high coefficients of determination; for the velocity measurement the minimum was R^2=0.998 and for the dispersion coefficient measurement the minimum was R^2=0.938.

The non-Gaussian shape of the peak in the disordered array (Fig. 4) is due to a defect in the channel immediately after the injection area. The injected plug of DNA must deform around the defect, resulting in a tail in the electropherogram. There is also a small peak of intensity at a distance slightly after the λ DNA peaks due to the presence of small fragments of DNA. These fragments could have been introduced from the original sample, or broken off from λ DNA by high shear flows during pipetting [30] or by photocleavage [31, 32]. The DNA fragments and imperfect injection result in deviations from Gaussian shaped electropherograms. Since our method for calculating the dispersion coefficient is

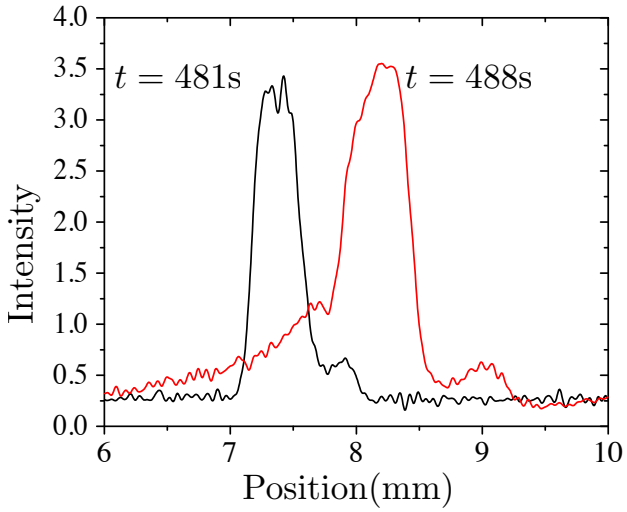

FIG. 4: (Color online) Overlaid electropherograms of λ DNA in the ordered array (black, $E = 6.9$ V/cm, $t = 481$ s) and in the disordered array (red, $E = 6.8$ V/cm, $t = 488$ s).

based on the growth of the FWHM, these imperfections are equivalent to background noise and do not lead to inaccuracies in the dispersion coefficient calculation. DNA velocity is calculated from the change in peak position with respect to time and is also unaffected by the non-Gaussian shape of the peaks.

III. THEORY

According to the two-state continuous-time random walk (CTRW) model [19], DNA undergoing electrophoresis in a post array is considered to be in one of two states: (i) colliding with a post for hold-up time t_H with no center of mass displacement ($x = 0$), or (ii) translation for time t_T over a random distance x. DNA transport is fully described by the first and second moments of the random variables t_H, t_T, and x. The dispersion coefficient of a single DNA size can be written as

$$2\bar{D}\left(\langle t_H\rangle + \langle t_T\rangle\right) = \sigma_x^2 + \bar{U}^2(\sigma_{t_H}^2 + \sigma_{t_T}^2) - 2\bar{U}\rho_{xt_T}, \tag{3}$$

where $\langle z\rangle$ represents the average of variable z and σ_z^2 is the variance in z. We must account for the space-time correlation, ρ_{xt_T}, defined as

$$\rho_{xt_T} = \langle xt_T\rangle - \langle x\rangle\langle t_T\rangle, \tag{4}$$

and estimated from the moving stage data. Values of the above variables were calculated from the distributions of the CTRW variables measured in single molecule experiments. We measured the hold-up time, t_H, from stationary stage experiments. The distribution of the distance between collisions, x, and the time between collisions, t_T, were measured from moving stage experiments. The velocity in the model is given by the distance traveled during one collision/translation cycle,

$$\bar{U} = \frac{\langle x \rangle}{\langle t_H \rangle + \langle t_T \rangle}. \tag{5}$$

IV. RESULTS AND DISCUSSION

A. Fabrication and Characterization

We directly measured the disorder of the array from a SEM image of a portion of the post array such as the ones in Fig. 3A and Fig. 3B. Using the Wiener-Khinchin theorem, we calculated the two dimensional autocorrelation function from the binary image of the array. The average intensity at a distance r from the origin of the autocorrelation function, $l(r)$, was given by the average intensity of pixels contained in an annulus of width 0.01 μm. Fig. 3C and Fig. 3D show the autocorrelation function of the ordered array and Fig. 3E and Fig. 3F show the radial intensity function. The large, blurry spots in the autocorrelation function in Fig. 3D indicate the variation in post spacing in the disordered array. The dispersion of the array was based on the width of the second peak in a plot of $l(r)$ versus r (Fig. 3E, 3F) following the work of Minc *et al.* [13].

Using this method we measured $s = 0.045$ and 0.352 for the ordered and disordered arrays respectively. For comparison, s ranges from 0.16 to 0.47 in magnetic bead arrays [13]. The measured values differ from the theoretical array dispersion due to limitations in the mask making process. Explicitly, the post positions on the mask are limited to a 2D lattice and cannot be placed with infinite precision. This limited spatial resolution resulted in additional order in the disordered arrays and also prevented the fabrication of a perfectly ordered array.

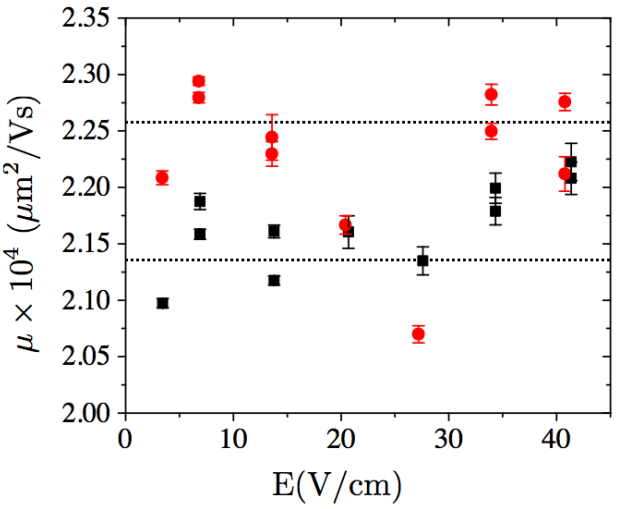

FIG. 5: (Color online) Electrophoretic mobility of λ DNA in the ordered array (black squares) and the disordered array (red circles) as a function of applied electric field. Error bars show the standard error for the fitting within a given experiment. Dashed lines show plus or minus one standard deviation from the mean of the data in this figure.

B. Mobility

The electrophoretic mobility measured in the 5-reservoir device is plotted in Fig. 5 as a function of the applied electric field. We also computed the mean of the mobility measurements for both arrays and all E and plotted dashed lines one standard deviation above and below the mean. We only observed a 3% deviation from the mean electrophoretic mobility over all electric fields, array geometries, and different experiments. This variance in the measured mobility is comparable to that measured for a single DNA size at a single electric field in microfluidic devices [5, 13, 17]. While the standard deviation of mobility for small DNA molecules in capillary electrophoresis is around 1.7% [33], the standard deviation of mobility for large DNA in TBE buffer can be as high as 4% [29]. In light of the standard deviations observed in previous experiments and the data in Fig. 5, there is no significant difference in mobility between the hexagonal ordered array and the disordered array. Also, the mobility does not depend on the applied electric field.

In the single molecule experiments, we determined the DNA mobility, μ, from the average passage time of DNA molecules across the fixed viewing window and we calculated the free

TABLE I: Summary of the velocity, $\bar{U}$, and dispersion coefficient, $\bar{D}$ in each experiment.

	Array Type	E	$\bar{U}$ (μm/s)	$\bar{D}$ (μm^2/s)
5-reservoir	ordered	6.9	15.0	28.9
2-reservoir	ordered	10	18.6	16.9
5-reservoir	ordered	13.8	29.5	56.2
5-reservoir	disordered	6.8	15.5	47.6
2-reservoir	disordered	10	19.0	18.5
5-reservoir	disordered	13.6	30.4	226

solution mobility, μ_0, from the DNA velocity between collisions. From the single molecule experiments at 10 V/cm, we found a dimensionless mobility, μ/μ_0, of 0.874 in the ordered array and 0.870 in the disordered array. These dimensionless mobilities are less than unity due to frequent long-lived DNA-post collisions.

As shown in Table 1, the values of the velocity measured from the single molecule experiments in the 2-reservoir device do not match the velocity measured in the 5-reservoir device. Day-to-day variations in the buffer, channel conditions, and environmental factors can lead to differences in the electro-osmotic flow (EOF), and thus in the measured DNA mobility [5]. If we assume that the variation in velocity between experiments comes from a difference in the electro-osmotic flow in the different devices, it is useful to write the electrophoretic mobility as a contribution from interactions with the post array, μ^o, and a contribution due to the EOF, $\mu_{\rm EOF}$:

$$\mu = \mu^o + \mu_{\rm EOF}. \tag{6}$$

The mobility due to interactions with the post arrays depends on the array type only. The EOF term is the same within an experiment but varies between the two sets of experiments. Thus, the difference in mobility, $\Delta\mu$, between the 2-reservoir device, μ_2, and 5-reservoir device, μ_5, for a single array type (ordered or disordered) could be explained by the change in the electro-osmotic flow, $\Delta\mu = \Delta\mu_{\rm EOF}$. We found that $\Delta\mu_{\rm EOF} = 0.36$ μm cm/Vs in the ordered array and $\Delta\mu_{\rm EOF} = 0.35$ μm cm/Vs in the disordered array. While these two values are not identical, they are within the experimental error.

To further investigate the difference between DNA electrophoresis in ordered and disordered arrays, we looked at the parameters of the continuous-time random walk model [19].

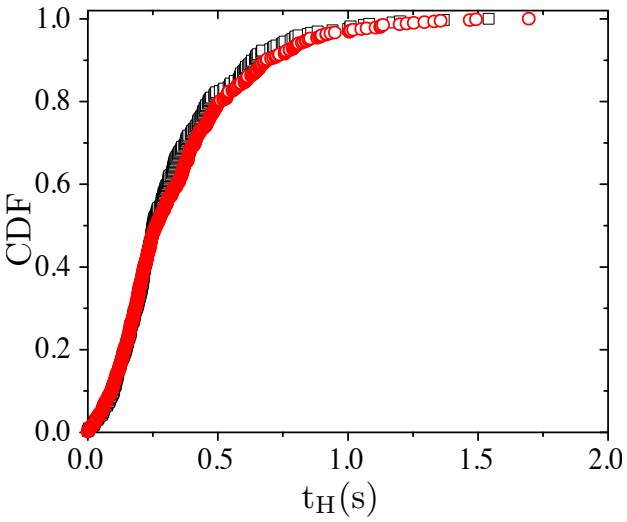

FIG. 6: (Color online) Cumulative distribution function (CDF) of the hold-up times for the ordered array (black squares) and the disordered array (red circles). The hold-up times are measured from single molecule videomicroscopy at a fixed position at 10 V/cm.

We measured the hold-up time under an applied electric field of 10 V/cm for 602 collisions in the disordered array and for 326 collisions in the ordered array and plotted the cumulative distribution function in Fig. 6. The two distributions are the same to within a 93.5% confidence level. The data follow the gamma distribution as was the case for DNA collisions with an isolated post [22] and in a nanofence geometry [20]. In the two-state CTRW model, computing the DNA velocity requires the mean hold-up time, while information on the full hold-up time distribution is important for determining the dispersion coefficient of a group of DNA molecules. The mean hold-up time is 0.32 s in the ordered array and 0.35 s in the disordered array. The mean hold-up times are similar because post size is the same in both arrays, and DNA molecules were rarely hung up on more than one post at a time at 10 V/cm. While the arrangement of the posts does affect the electrical forces acting on the molecule, the differences in post arrangement do not lead to an appreciable difference in the hold-up time once a DNA molecule is engaged with a post.

From the stationary stage data we were able to estimate the collision probability for the DNA in each of the arrays at 10 V/cm from the number of collisions observed as molecules passed through the viewing window divided by the number of rows in the viewing window. We found $\rho_c = 0.052$ in the ordered array and $\rho_c = 0.081$ in the disordered array. The collision

probability in the disordered array matches collision probabilities measured in magnetic bead arrays [13]. Both collision probabilities are in the range of ρ_c measured in uniform electric field simulations [16].

Using these collision probabilities as the probability for colliding in each row of posts, the cumulative distribution function (CDF) of the distance between collisions, x, would be

$$\mathrm{CDF}(\rho_c, x) = 1 - \exp\left(\rho_c x\right). \tag{7}$$

We plotted this model for each array as the solid lines in Fig. 7. The decreased collision probability in the ordered array is due to fact that alternating rows of posts are offset by 2.5 μm. This large lateral offset reduces the collision probability in alternating rows because the molecule is unable to diffuse lateral to the applied electric field to collide with the first few offset rows. This qualitative explanation is supported by single molecule data for the the distance between collisions in the ordered array, which are shown in the inset of Fig. 7. Because some posts are unavailable for collision in the ordered array we see a lower collision probability than in the disordered array for short distances. As we will explain later, the collision probabilities for the ordered array and disordered array converge for long distances.

We must observe two collisions for a single molecule to be able to measure the distance between collisions. In the stationary stage experiment the majority of the molecules pass through the viewing window without making two collisions. In those experiments, the distance between collisions can be no more than 70 μm and, unsurprisingly, we find that the measured distribution is biased towards small distances between collisions. To increase the viewing window to 216 μm, we captured video data while moving the stage to follow individual DNA molecules using the protocol described above. To remove any bias in the measured distribution, we defined a cut-off distance of 180 μm. Any molecule included in the distribution must be observed for at least 180 μm after it makes its first collision. The cumulative distribution function for this unbiased distance between collisions is shown for each array in Fig. 7. As we can see, λ DNA makes frequent collisions in both of the arrays. Over short distances, the CDF extrapolated from the stationary stage experiments matches the CDF measured in the moving stage experiments.

Due to the large offset between consecutive rows in the ordered post array, DNA molecules cannot make a collision with every row. However, if the molecule travels long enough in the ordered array without colliding, it will diffuse such that its location after a previous

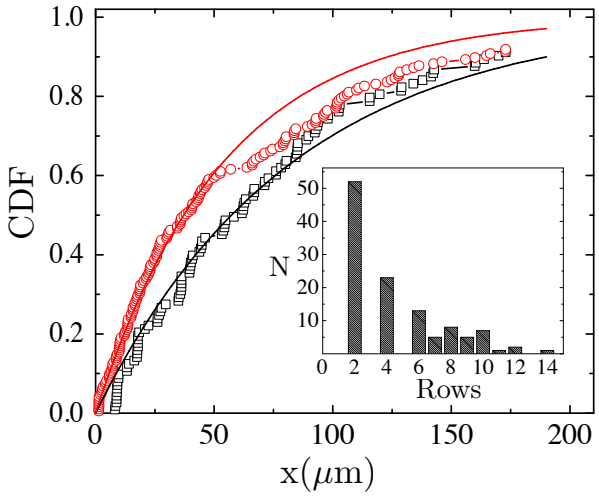

FIG. 7: (Color online) The cumulative distribution function (CDF) of the distance between collisions for the ordered array (black squares) and the disordered array (red circles). The solid lines show the CDFs predicted by Eq. 7. Molecules included in the data set were tracked at least 180 μm after their initial collision. For the ordered array, 91.2% (103/113) of the molecules collide within 180 μm while for the disordered array, 91.8% (179/195) of the molecules collide within 180 μm. The inset shows the number of collisions, N, for a given number of rows between collisions observed at each distance in the stationary stage experiment in the ordered array.

collision is uncorrelated to its current position. For this to occur, the molecule must diffuse over a distance equal to the distance from the edge of one post (its initial location after the collision) to the center of the offset row of posts. In a hexagonal array of 1 μm diameter posts with 5 μm spacing, this is a distance of $a = 2$ μm. The diffusion time is then $t_{\text{diff}} = a^2/2D_0$, where the diffusion coefficient of λ DNA is $D_0 = 0.47$ μm^2/s [34]. In this time, the molecule travels a distance of 84.7 μm at the free solution mobility at $E = 10$ V/cm. The data in Fig. 7 show that the two CDFs converge after this distance. While the collision probabilities over short distances depend strongly on the order of the array, they become indistinguishable at long distances.

C. Plate Height

While the DNA velocity and electrophoretic mobility depend only on the first moment of the hold-up time and distance between collisions, the dispersion coefficient, and thus the plate height, depends on the second moment of these random variables as well. The second moment captures molecule to molecule variability, which gives rise to macroscopic band broadening. As discussed above, the hold-up time distributions (Fig. 6) and distance between collisions distributions (Fig. 7) measured from single molecule experiments at $E =$ 10 V/cm show only a slight dependence on array order. From these results, and the time between collisions measured in the moving stage experiments, we calculated the dispersion coefficient in Table 1 using the CTRW model. We note that the dispersion coefficients for the 2-reservoir device do not account for any sources of dispersion in the channel not due to DNA-post collisions and thus represent a theoretical minimum. In the 5-reservoir experiments, we calculated the dispersion coefficient in each array from the growth of λ DNA peak width. Measurement of the dispersion coefficient from macroscopic variables includes all sources of band broadening that are present during transport in the device. As in the single molecule case, the dispersion coefficient is higher in the disordered array. Since the 5-reservoir experiments involve many possible sources of band broadening, it is unsurprising that they exhibit a higher dispersion coefficient.

Experiments conducted in the 5-reservoir device allowed us to measure the dispersion coefficient at several different applied electric fields. We found that the dispersion coefficient is always higher in the disordered array, and increases with increasing electric field. This qualitative behavior agrees with experiments in magnetic bead arrays [8], experiments in ordered arrays [17], and in simulations of λ DNA in ordered arrays [19, 39]. From the macroscopic measurements of the DNA velocity, $\bar{U}$, and dispersion coefficient, $\bar{D}$, we calculated the plate height, $H = 2\bar{D}/\bar{U}$, and plotted it in Fig. 8. The plot of plate height versus applied electric field in Fig. 8 shows that plate height in the ordered array is constant over the range of electric fields studied; however, plate height in the disordered array is not constant.

Simple scaling laws for the CTRW parameters suggest that H should be independent of E. We will assume that $t_H \sim E^{-1}$, which has been verified experimentally [14, 35]. We also propose that $t_T \sim E^{-1}$ which is equivalent to assuming that the free solution velocity scales

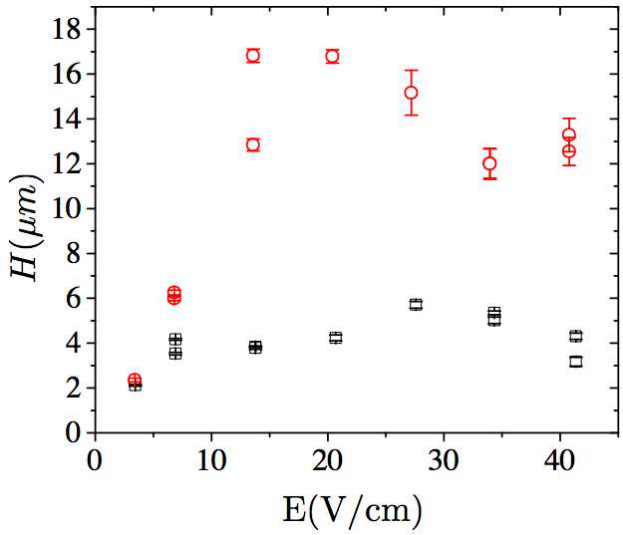

FIG. 8: (Color online) Plate height as a function of electric field for the ordered array (black squares) and the disordered array (red circles). Error bars show the standard error of the plate height in a given experiment. The dispersion coefficient is calculated from the band broadening measured in the channel scanning experiments.

with E. As shown in Fig. 5, $\mu \sim E^0$ and thus $\bar{U} \sim E$. We can write the DNA velocity as

$$\bar{U} = \frac{\langle x \rangle}{\langle t_H \rangle + \langle t_T \rangle}. \tag{8}$$

Since both times scale with E^{-1}, $\langle x \rangle$ must be independent of the applied electric field. This is equivalent to stating that the collision probability is independent of E, a common assumption in CTRW models [36, 37] supported by experimental evidence [13, 16]. Using $t_H \sim E^{-1}$ and $\rho_c \sim E^0$ we find that $\bar{D} \sim E$ from Taylor-Aris dispersion theory [38]. Thus, we expect that the plate height is independent of E. Indeed, this is true in the ordered array. However, the plate height in the disordered array is not constant across the range of E.

The two-state CTRW model lends insight into the sources of band broadening in post array devices [19]. We can express the plate height in general as

$$H = \frac{\sigma^2_{x-\bar{U}t_T}}{\langle x \rangle} + \frac{\bar{U}^2 \sigma^2_{t_H}}{\langle x \rangle} \tag{9}$$

where the first term is the contribution to H due to fluctuations in the transport between collisions and the second term is due to fluctuations in the hold-up time of a collision. We

can already exclude the fluctuations in the distance between collisions as the source of the higher plate height in the disordered array since the CDF for the distance between collisions in Fig. 7 is similar for the ordered and disordered array for the large values of x that would dominate the variance. However, we also need to consider fluctuations in the time required to traverse the distance x. Convective transport between collisions is driven by the electric field. The posts are insulating, so the electric field lines bend around the posts leading to the curved field lines shown in Fig. 1. The field lines are more irregular in the disordered array, whereupon we might anticipate that the fluctuations in the time between collisions for a give distance x will be greater in the disordered array. However, the calculated electric field lines shown in Fig. 1 lead us to suspect that the difference in the local electrophoretic velocities are a small contribution to the plate height in this relatively sparse array.

If the first term in Eq. 9 is similar for the ordered and disordered array, the major contribution to H in the disordered array must be increased fluctuations in the hold-up time. We propose that this increase with electric field in the disordered array is caused by the non-uniform placement of the posts. Based on our previous Brownian dynamics simulations in a more dense ordered array, fluctuations in the hold-up time term are related to the extension of the molecule during collision [19]. Specifically, once the molecule is extended enough to interact with two rows of posts during a collision, the plate height increases dramatically. Figure 1 shows a schematic of DNA colliding with the posts of each array and includes an example of a multiple post collision. Because DNA does not collide with consecutive rows in the ordered array (inset, Fig. 7), the minimum extension for a multiple post collision in the ordered array is equal to twice the row spacing, 8.7 μm. Note that the latter value is a very conservative estimate, since the unraveling chain needs to have sufficient relaxed DNA at its head to initiate a second collision. In the disordered array, the extension required for multiple post collisions varies depending on the location of the posts. Thus, multiple post collisions can occur even at relatively low extension in regions of the post array where the density of posts is high. Multiple post collisions have a much larger mean hold-up time than single post collisions; therefore, a t_H distribution in an array where both types of collisions can occur has a much higher variance than a t_H distribution where only single post collisions are possible. As E increases, the extension of the molecule during collision increases. At $E > 10$ V/cm, the DNA extension is great enough to allow frequent multiple post collisions in the disordered array, which we believe results in the increase in

H. Owing to the rapid motion of the chain at higher electric fields, it is difficult to confirm our hypothesis with single molecule measurements. The requisite extension in the ordered array for multiple post collisions occurs at a much higher E that is not reached in our single molecule experiments. As a result, the ordered array follows the models for collision with an isolated post [36, 38], where H is independent of E.

V. CONCLUSIONS

In the present contribution, we measured the electrophoretic mobility and dispersion coefficient of a single size of DNA molecules in an ordered hexagonal array of posts and a disordered array of posts from two different types of experiments. Video microscopy experiments revealed micro-transport properties such as the hold-up time of a collision and the distance traveled between collisions. Although macroscopic measurements of a group of DNA in the array do not allow as much insight into the details of the transport process, they do allow us to measure mobility and dispersion over a large range of applied electric fields. Both types of experiments compare DNA dynamics in an ordered and disordered geometry in a single integrated device that isolates the effect of array order on transport.

To improve a separation, we must increase the separation resolution, which is proportional to the difference in mobility and inversely proportional to the square root of the plate height. Based on the data presented here, the array type does not alter the DNA mobility. However, the plate height does depend on the array type. The increased plate height in the disordered array leads to greater band broadening in the device and to poorer separation resolution. We found that a lower applied electric field results in less band broadening and therefore a higher separation resolution. This result is in agreement with previous experiments of an electrophoretic separation of 48.5 kbp DNA and 2.7 kbp DNA in a sparse ordered array [5] and Brownian dynamics simulation of the separation of 169 kbp DNA and 48.5 kbp DNA [39].

The work presented here shows that DNA separation by rope-over-pulley collisions in a 2D device is optimized in an ordered geometry. Improvement in the separation due to reduced band broadening in an ordered, 2D geometry also occurs in liquid chromatography [40, 41]. DNA separation by Ogston sieving is possible in 3D geometries formed by self-assembly of colloid solutions [42]. While there has not been a study of the role of order in

dc field separation in a colloidal crystal, a study of long DNA separation under a pulsed electric field in a 3D colloidal array found that an ordered matrix improved the separation resolution over a disordered matrix [43]. We anticipate that dc electric field separations in 3D colloidal arrays will also benefit from increased array order, similar to the results for protein chromatography in colloidal crystals [44].

Acknowledgments

This work was supported by National Science Foundation Grant No. CBET-0642794. Portions of this work were performed in the University of Minnesota Nanofabrication Center, which receives partial support from the NSF though the NNIN, and in the Institute of Technology Characterization Facility, University of Minnesota, a member of the NSF-funded Materials Research Facilities Network (www.mrfn.org).

---

[1] N. Kaji, Y. Tezuka, Y. Takamura, M. Ueda, T. Nishimoto, H. Nakanishi, Y. Horiike and Y. Baba, Anal. Chem., **76**, 15–22 (2004).

[2] Y. C. Chan, Y. K. Lee and Y. Zohar, J. Micromech. Microeng., **16**, 699–707 (2006).

[3] J. Shi, A. P. Fang, L. Malaquin, A. Pepin, D. Decanini, J. L. Viovy and Y. Chen, Appl. Phys. Lett., **91**, 153114 (2007).

[4] R. Ogawa, N. Kaji, S. Hashioka, Y. Baba and Y. Horiike, Jpn. J. Appl. Phys., **46**, 2771-2774 (2007).

[5] J. Ou, S. J. Carpenter and K. D. Dorfman, Biomicrofluidics, **4**, 013203 (2010).

[6] J. Ou, M. N. Joswiak, S. J. Carpenter and K. D. Dorfman, J. Vac. Sci. Technol. A, **29**, 011025 (2011).

[7] P. S. Doyle, J. Bibette, A. Bancaud and J. L. Viovy, Science, **295**, 2237 (2002).

[8] N. Minc, C. Futterer, K. D. Dorfman, A. Bancaud, C. Gosse, C. Goubault and J. L. Viovy, Anal. Chem., **76**, 3770-3776 (2004).

[9] C. Heller, T. Duke and J. L. Viovy, Biopolymers, **34**, 249-259 (1994).

[10] W. D. Volkmuth, and R. H. Austin, Nature, **358**, 600–602 (1992).

[11] N. P. Teclemariam, V. A. Beck, E. S. G. Shaqfeh, and S. J. Muller, Macromolecules, **40**,

3848–3859 (2007).

[12] G. I. Nixon, and G. W. Slater, Phys. Rev. E, **50**, 5033–5038 (1994).

[13] N. Minc, P. Bokov, K. B. Zeldovich, C. Futterer, J.-L. Viovy, and K. D. Dorfman, Electrophoresis **26**, 362–375 (2005).

[14] G. C. Randall, and P. S. Doyle, Macromolecules, **39**, 7734–7745 (2006).

[15] P. D. Patel, and E. S. G. Shaqfeh, J. Chem. Phys., **118**, 2941–2951 (2003).

[16] A. Mohan, and P. S. Doyle, Phys. Rev. E, **76**, 040903(R) (2007).

[17] J. Ou, J. Cho, D. W. Olson and K. D. Dorfman, Phys. Rev. E, **79**, 061904 (2009).

[18] D. W. Olson, J. Ou, M. Tian, and K. D. Dorfman, Electrophoresis, **32**, 573–580 (2011).

[19] D. W. Olson, S. Dutta, N. Laachi, M. Tian, and K. D. Dorfman, Electrophoresis, **32**, 581–587 (2011).

[20] S. G. Park, D. W. Olson, and K. D. Dorfman, Lab Chip, **12**, 1463–1470 (2012).

[21] A. Larsson, C. Carlsson, M. Jonsson, and B. Albinsson, J. Am. Chem. Soc., **116**, 8459–8465 (1994).

[22] M. N. Joswiak, J. Ou, and K. D. Dorfman, Electrophoresis, **33**, 1013–1020 (2012).

[23] O. A. Hickey, J. L. Harden, and G. W. Slater, Phys. Rev. Lett., **102**, 108304 (2009).

[24] R. S. Madabhushi, Electrophoresis, **19**, 224–230 (1998).

[25] G. C. Randall, and P. S. Doyle, Phys. Rev. Lett., **93**, 058102 (2004).

[26] G. C. Randall, and P. S. Doyle, Macromolecules, **38**, 2410–2418 (2005).

[27] A. E. Nkodo, J. M. Garnier, B. Tinland, H. Ren, C. Desruisseaux, L. C. McCormick, G. Drouin, and G. W. Slater, Electrophoresis, **22**, 2424–2432 (2001).

[28] J. Mathé, J.-M. Di Meglio, and B. Tinland J. Colloid Interf. Sci., **316**, 831–835 (2007).

[29] N. C. Stellwagen, C. Gelfi, and P. G. Righetti, Biopolymers, **42**, 687–703 (1997).

[30] R. T. Kovacic, L. Comal, and A. J. Bendich, Nucleic Acids Res., **23**, 3999–4000 (1995).

[31] S. Gurrieri, K. S. Wells, I. D. Johnson, and C. Bustamante, Anal. Biochem., **249**, 44–53 (1997).

[32] B. Akerman, and E. Tuite, Nucleic Acids Res., **24**, 1080–1090 (1996).

[33] E. Stellwagen, and N. C. Stellwagen, Electrophoresis, **23**, 2794–2803 (2002).

[34] D. E. Smith, T. T. Perkins, and S. Chu, Macromolecules, **29**, 1372–1373 (1996).

[35] W. D. Volkmuth, T. Duke, M. C. Wu, R. H. Austin, and A. Szabo Phys. Rev. Lett., **72**, 2117–2120 (1994).

[36] N. Minc, J.-L. Viovy, and K. D. Dorfman, Phys. Rev. Lett., **94**, 198105 (2005).

[37] A. Mohan, and P. S. Doyle, Macromolecules, **40**, 8794–8806 (2007).

[38] K. D. Dorfman, and J.-L. Viovy, Phys. Rev. E, **69**, 011901 (2004).

[39] J. Cho, and K. D. Dorfman, J. Chromatogr. A, **1217**, 5522–5528 (2010).

[40] J. Billen, P. Gzil, N. Vervoort, G. V. Baron and G. Desmet, J. Chromatogr. A, **1073**, 53-61 (2005).

[41] M. De Pra, W. Th. Kok, J. G. E. Gardeniers, G. Desmet, S. Eeltink, J. W. van Nieuwasteele and P. J. Schoenmakers, Anal. Chem., **78**, 6519-6525 (2006).

[42] Y. Zeng, and D. J. Harrison, Anal. Chem., **79**, 2289–2295 (2007).

[43] N. Nazemifard, L. Wang, W. Ye, S. Bhattacharjee, J. H. Masliyah, and D. J. Harrison, Lab Chip, **12**, 146–152 (2012).

[44] D. S. Malkin, B. Wei, A. J. Fogiel, S. L. Staats, M. J. Wirth, Anal. Chem., **82**, 2175–2177 (2010).